# We are IntechOpen,
## the world's leading publisher of Open Access books
## Built by scientists, for scientists

**6,900**
Open access books available

**185,000**
International authors and editors

**200M**
Downloads

**154**
Countries delivered to

Our authors are among the

**TOP 1%**
most cited scientists

**12.2%**
Contributors from top 500 universities

CLARIVATE ANALYTICS
**BOOK CITATION INDEX**
INDEXED

**WEB OF SCIENCE™**

Selection of our books indexed in the Book Citation Index
in Web of Science™ Core Collection (BKCI)

## Interested in publishing with us?
## Contact book.department@intechopen.com

# Practical Methods
# for Crack Length Measurement and
# Fatigue Crack Initiation Detection
# Using Ion-Sputtered Film and Crack Growth
# Characteristics in Glass and Ceramics

Gang Deng[1,2] and Tsutomu Nakanishi[1]
*[1]Faculty of Engineering, University of Miyazaki,*
*[2]State Key Lab of Mechanical Transmission, Chongqing University*
*[1]Japan*
*[2]China*

## 1. Introduction

A crack length measurement method is very important in the investigation of the fatigue crack growth characteristics of a material and in the evaluation of the fatigue strength of a machine element. Many crack length measurement methods have been proposed. Brown et al. (1966) and Nishitani et al. (1985) measured crack length through the changes in the displacement and compliance of the test piece. Ashida et al. (1996) and Nakai et al. (1989) investigated the changes in electrical properties around a crack during its growth. Lee et al. (1985) and JSME (1986) recommended estimating the crack length from the opening or closing displacement of a crack. In addition, crack length can also be measured by using an optical microscope, an optical grid technology (Bucci et al., 1972, Maustz et al., 1976, James et al., 1981), an acoustic emission method (Masuyama et al., 1994) and an ultrasonic method (Shimada et al., 1983). However, the methods proposed up to now require specific measuring apparatuses and complex calculation processes for crack length, and are applicable to long cracks several millimeters in length, not to small cracks shorter than 1mm in length or cracks with a high growth rate. In addition to the above-mentioned methods, a thin metal film, such as a crack gauge (e.g., KV-25B manufactured by Kyowa Co.), has been used for crack length measurement and fatigue crack initiation detection in some machine elements, such as gears, where cracks are up to several millimeters in length (Deng et al., 1991). Since this metal film is formed on a plastic base film with a thickness of about several tens of micrometers, there is a relatively large error between the actual and measured crack lengths. Increasing the measurement accuracy of the film can only be achieved by decreasing the thicknesses of the metal and plastic base films.

An ion-sputtering device, widely used in a scanning electron microscopy system, is a coating device used to form a nanoscale-thickness metal film on a surface. In this chapter, we introduce methods for crack length measurement using an ion-sputtered film, which are considered as ideal and practical methods applicable to micro-cracks or small cracks in glass

and ceramics as well as metals. The measurement principle and measuring system are very simple. As an application of the ion-sputtered film to crack length measurement, cracks in soda-lime glass and alumina ceramics were measured and the microcrack growth characteristics of these materials were clarified. In addition, an ion-sputtered film was also applied to the detection of fatigue crack initiation, and a very small crack that initiated from the notch surface of the acrylic test piece during the fatigue test was detected..

## 2. Crack length measurement using grid pattern ion-sputtered film

### 2.1 Measurement principle

Conductive films have been used for crack length measurement. Ogawa et al. (1991a, 1991b) and Nakamura et al. (1993) utilized carbon films to measure the crack length on ceramic surfaces, but their methods are not widely used because the presented relationship between crack length and the resistance of the film is applicable only to the film of specific dimensions. A crack gauge is also a sensor for measuring crack length and has been used to measure the crack length of gears (Deng et al., 1991), but the measurement precision is not satisfied owing to the thickness of the gauge.

An ion-sputtering device, as shown in Figure 1, is commonly used to fabricate a conductive with a thickness of several tens of nanometers. The application of an ion-sputtered film to crack length measurement would contribute to increasing the crack length measurement precision.



Fig. 1. Ion-sputtering device

The electrical resistance $R$ of a conductive film is expressed by

$$R = \rho \frac{l}{wt} \tag{1}$$

where $l$, $w$ and $t$ are the length, width and thickness of the film, respectively. $\rho$ is the specific resistance of the film material. However, expression (1) is applicable only to a film with a simple shape. If there is a crack of length $a$ across the film, attention should be paid on the fact that the electrical resistance cannot be calculated simply by substituting the width $w$ of expression (1) with the residual width $w$-$a$; the theoretical expression for the electric resistance of a cracked film is nearly impossible. However, if the length of the film is very large compared with the width of the film, indicating that the shape of the film is similar to

Practical Methods for Crack Length Measurement and Fatigue Crack Initiation Detection
Using Ion-Sputtered Film and Crack Growth Characteristics in Glass and Ceramics
105

that of a grid whose length $l$ is very larger than its width $w$, the electric resistance will not change before the crack entirely cuts off the film; the electric resistance is expressed by the following expression (Ogawa et al., 1991a).

$$R = \begin{cases} \text{constant} & a \neq w \\ \infty & a = w \end{cases} \qquad (2)$$

Thus, at the instant when a crack grows across the film with a grid shape, the electric resistance of the film will increase to infinity and the complex calculation of the electric resistance of the ion-sputtered film with a crack can be avoided; referring to the crack gauge, a grid pattern ion-sputtered film should be available for crack length measurement (Deng et al., 2006). The electric resistance of the grid pattern ion-sputtered film will increase owing to crack growth, crack length can be determined by counting the number of the increasing steps in the electric resistance and measuring the positions of the grids after or before an experiment.

## 2.2 Bending test piece and crack length measurement

To investigate the precision of the crack length measurement method using a grid pattern ion-sputtered film, three-point bending fatigue tests for acrylic test pieces were performed. Figure 2 shows the loading method, the test piece and the grid pattern ion-sputtered film. In the experiment, first, a notch was introduced into the test piece to easily introduce the fatigue crack from the notch under a cyclic load. The crack growth experiment was performed under a cyclic load for a slow crack growth. The thickness of the grid pattern ion-sputtered film was about 10nm, the grid width was 0.2mm, and the interval between two grids was 0.1mm. The supporting span was 80mm, and the width and thickness of the test piece were 20mm and 10mm, respectively. The cyclic load was a sine wave of 10Hz and the load ratio ($P_{min}/P_{max}$) was approximately 0.02. A very simple measurement system used for recording the electrical resistance, which consists of a DC power source, a variable resistor and a voltmeter, is shown in Figure 3. The supply voltage was approximately 1-2V, the supply voltage and variable resistor were adjusted for a current below 100mA. The voltage on the film during the fatigue test was recorded by a data recorder. The sampling speed for the voltage was 80Hz.
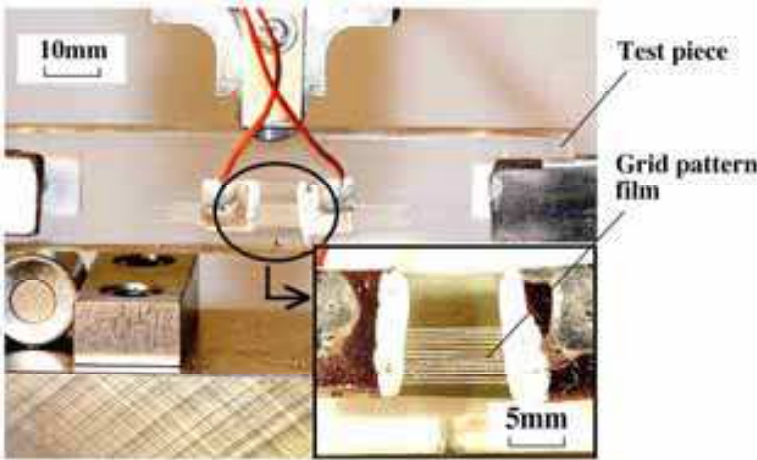


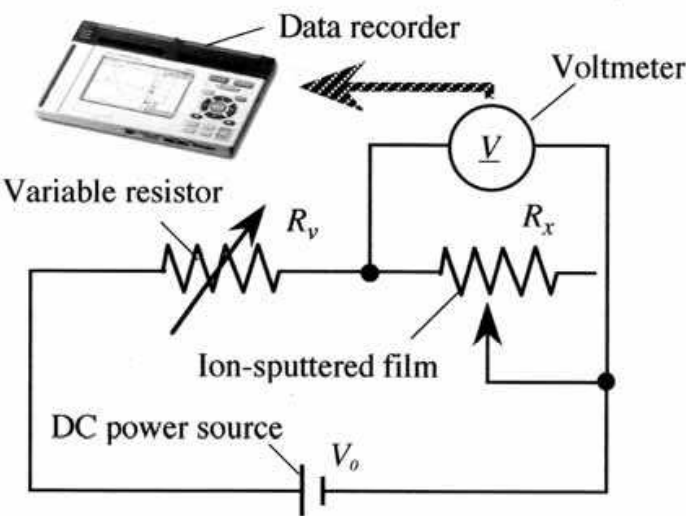Fig. 2. Test piece and grid pattern ion-sputtered film

Fig. 3. Measurement system for the electrical resistance of ion-sputtered film

## 2.3 Precision of crack length measurement with grid pattern ion-sputtered film

The change in the voltage of the grid pattern film during crack propagation is shown in Figure 4. Although fluctuations in voltage signals due to the deformation of the film and the sampling error were observed, a distinct staircase pattern was recorded for the electric resistance. Considering the characteristic of the electric resistance change for a cracked grid as expressed in expression (2), the increasing step in Figure 4 shows the instant of grid snapping. From the positions of the grids that can be measured with an optical microscope before or after an experiment with a very high precision, the crack length at the instant of the increasing step can be accurately estimated. The precision of this method depends on the film thickness and the speed of the measuring system in response to the crack growth. Since the recorded signal upturns vertically and the film is extremely thin, this method can intermittently measure cracks with a very high precision at the instant of grid snapping.
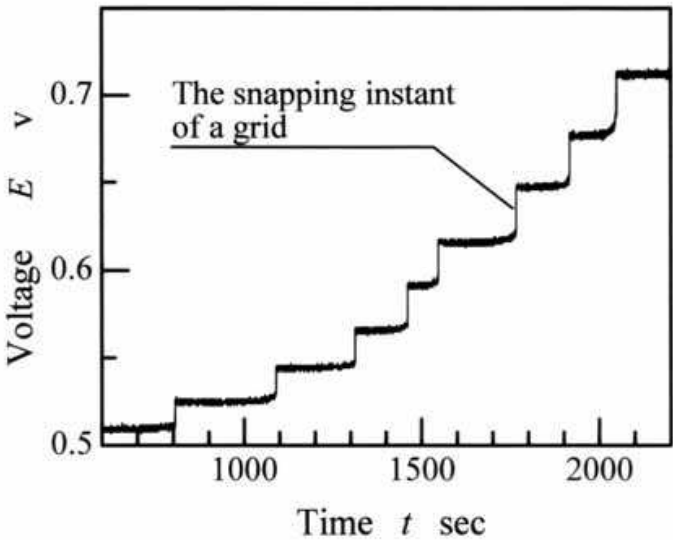


Fig. 4. Change in voltage of grid pattern film during crack propagation

For the application of the crack length measurement method using a grid pattern film to a rapidly growing crack, a fine-pitch grid pattern ion-sputtered film is desirable. Scribing the film using a sharp scriber tip, as shown in Figure 5, can produce grids of 25μm width and 50μm pitch. A film with 40 grids was fabricated and applied to a fatigue test. The change in the voltage of the film during crack propagation is shown in Figure 6, and 40 steps are identified clearly, indicating that 40 points of crack length can be obtained. Tokunaga et al. (2007) have succeeded in fabricating a grid pattern film using an excimer laser micromachining technology where the grid width is about 13μm and the pitch is 20μm for the measurement of cracks in ceramics.
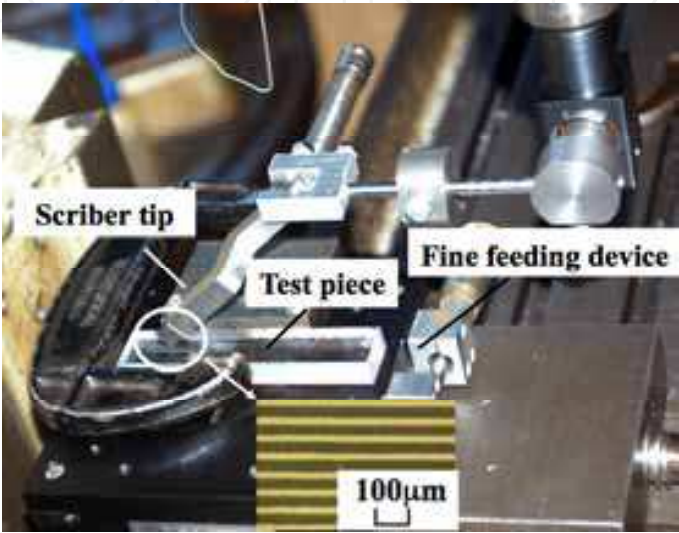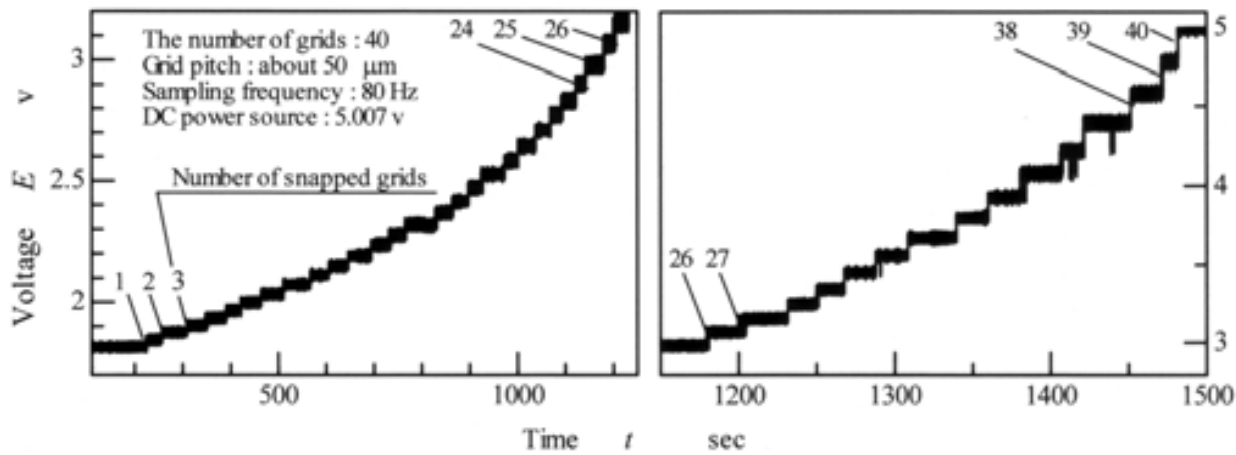


Fig. 5. Fabrication of fine grid film using scriber tip



Fig. 6. Change in voltage of fine grid pattern film during crack propagation

## 3. Crack length measurement using rectangular ion-sputtered film

Although the grid pattern ion-sputtered film can measure crack length with a high precision, the crack length cannot be determined continuously. In addition, an isolation film is necessary for the application of the grid pattern film to a conductive surface; the

formation of the grid pattern without destroying the isolation film would be very difficult. Thus, for measuring the crack length continuously and applying the ion-sputtered film to a conductive surface, such as a metal surface, a rectangular ion-sputtered film is desirable.

### 3.1 Calculation of electric resistance of cracked metal film

In the case of a cracked film under electric potential difference, the feature of electron flow around the crack, which is similar to that of stress concentration, is shown in Figure 7, and the electric resistance calculation becomes very complex. Ogawa et al. (1991a, 1991b) calculated the electric resistance of an across-cracked carbon film by FEM analysis and presented an approximating formula for the electric resistance of a regulated film where the crack length is in the range of 0.2-0.8$w$ ($w$ is the film width along the crack growth direction). Generally, the film width is several millimeters; thus, it is difficult to calculate the electric resistance of a film with a micro-crack shorter than 1mm using Ogawa's formula.
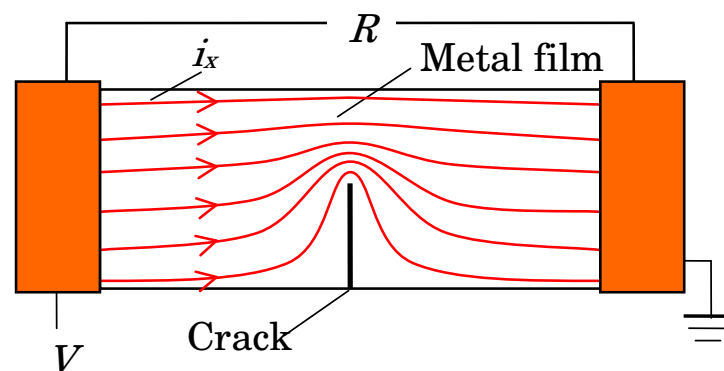


Fig. 7. Electron flows around crack

Electrothermal FEM is a practical method for calculating the electric resistance of the film with a crack (Deng et al., 2007). For example, when the mesh of a rectangular metal film and the boundary condition, shown in Figure 8, are prepared, the current density $i_x$ of each element can be obtained by FEM analysis. The total current in the $x$ direction can be calculated by integrating the current of each element, and the electric resistance can be obtained through the total current and electric potential difference on the basis of the law of ohm. The effect of the element size in FEM analysis on the calculation precision was investigated. Figure 9 shows the relationship between the calculated electric resistance and the number of elements for FEM analysis. Under the conditions that the length $l$ of the film is 20.8mm, the width $w$ of the film is 10.4mm and the crack length $a$ is 0.4$w$, the electric resistance approaches a constant value when the number of elements is more than 5000. It is strongly recommended that the change in the calculated electric resistance with the increase in the number of elements should be investigated, and that an appropriate number of elements should be chosen. Many software programs, such as ANSYS and Marc, are available for electrothermal analysis.

Figure 10 indicates the electric resistance of a cracked ion-sputtered film on an acrylic piece, where crack length was measured using an optical microscope. The difference between the electric resistances obtained by measurement and FEM analysis is only 2-3%; thus, it can be considered that the electric resistance of a cracked film is calculated correctly by FEM analysis.
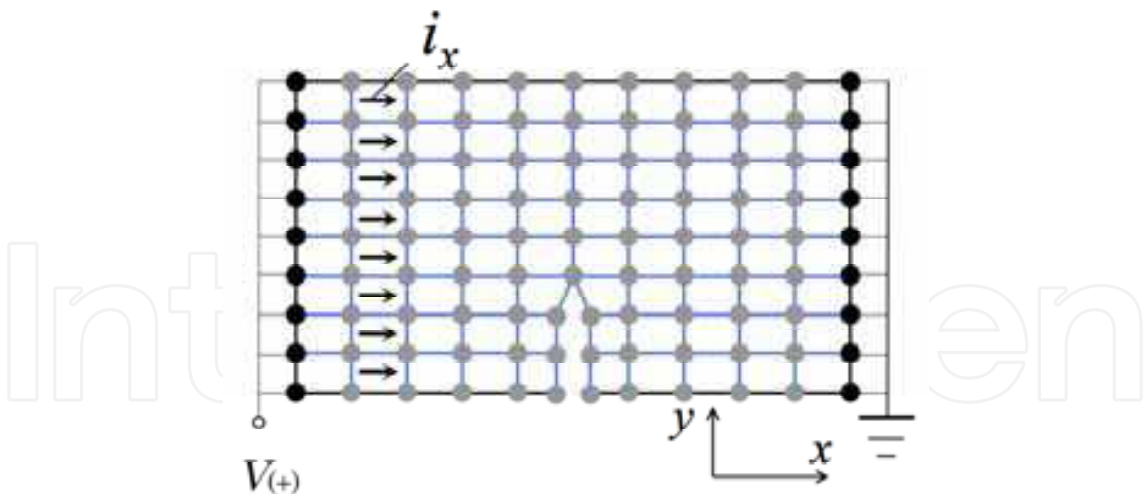
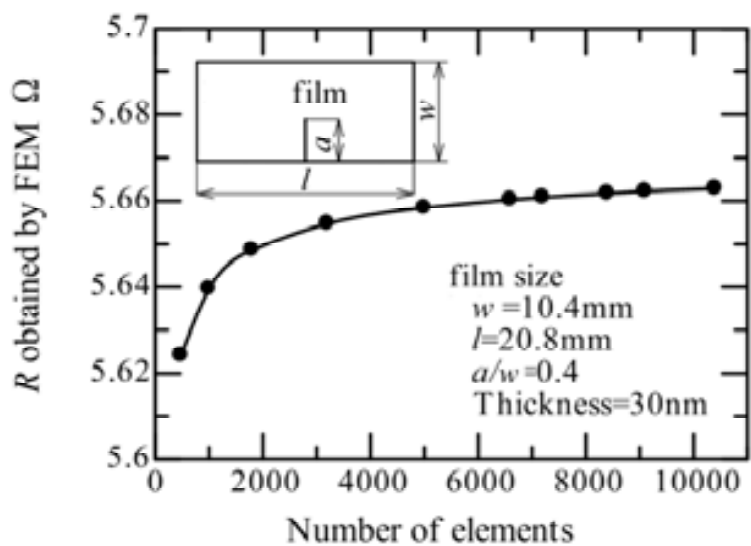Fig. 8. Mesh of cracked film and boundary condition for electro-thermal FEM analysis



Fig. 9. Electric resistance value obtained under different number of elements

Despite the many approaches that can be used to find the expression for the relationship between the electric resistance and the crack length from 0 to the film width, a satisfactory expression was not obtained. Finally, considering practicability, the following expression is introduced to show the relationship in the crack length range from 0 to a portion of the film width.

$$R = R_0 + ca^b \qquad (3)$$

Here, $R$ ($\Omega$) is the electric resistance of the cracked film, $a$ is the crack length (mm), $R_0$ ($\Omega$) is the electric resistance when $a=0$, and $c$ and $b$ are constants. Many calculations were carried out to determine the values of $b$ for the various dimensions of the films. The results of the calculations revealed that $b$ depends on the shape of the film. Figure 11 shows the values of $b$ at different ratios of the film length $l$ to the film width $w$. In the $l/w$ range from 2.0 to 3.5, constant $b$ is approximately equal to 2.268 on average.
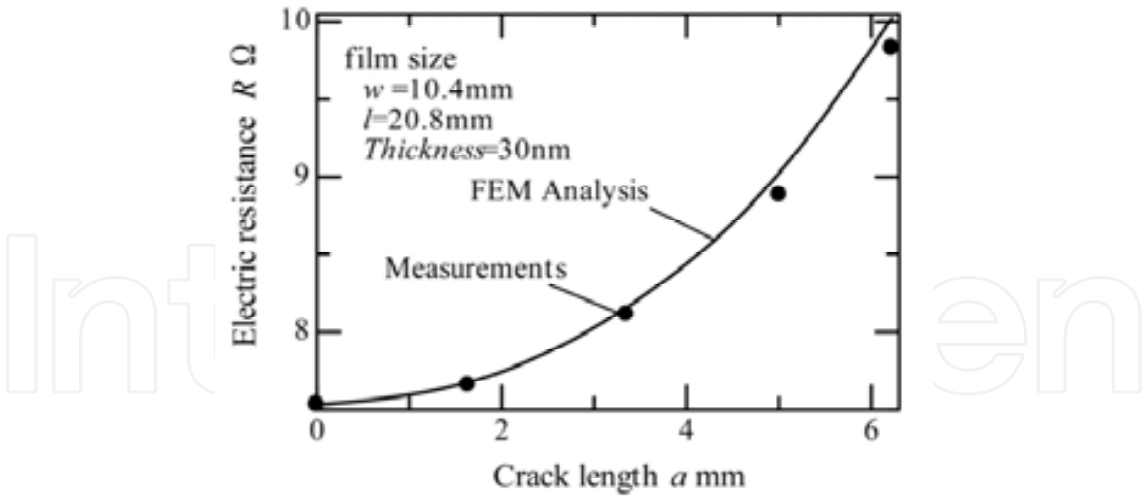
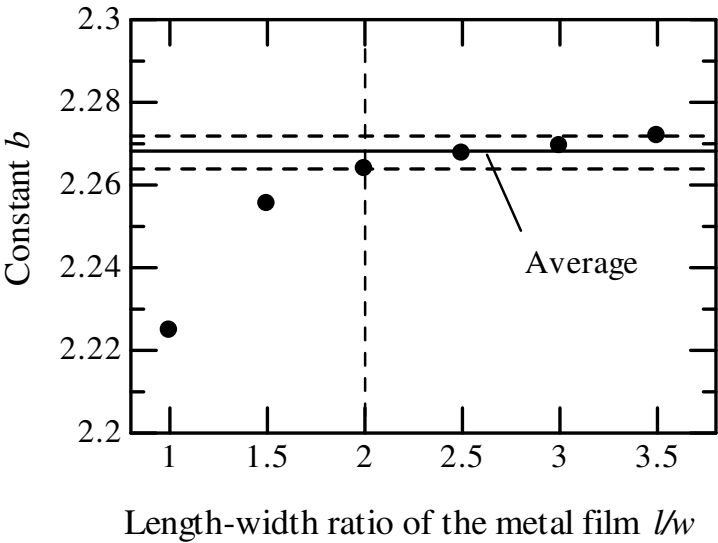Fig. 10. Electric resistance obtained by measurement and FEM analysis



Fig. 11. Values of *b* under different shape of the film

On the other hands, *c* can be determined by stopping the experiment before the crack entirely cuts off the film, measuring the crack length $a_e$ using an optical microscope, and substituting the electric resistance $R_e$ and crack length $a_e$ into expression (3). Several ion-sputtered films were used to verify the accuracy of expression (3). On the basis of the good agreement between the crack length estimated with expression (3) and measured using an optical microscope, the following expression is considered practical for estimating the electric resistance of a cracked film.

$$R = R_0 + ca^{2.268} \quad (0 \le a \le 0.6w, \ 2.0 \le \frac{l}{w} \le 3.5) \tag{4}$$

However, the physical meaning of expression (4) has not yet been clarified, and such an expression is only a curve-fitting formula and should be applicable to the condition shown in expression (4). Although this approximating expression can calculate the electric

resistance of a cracked film in a specific crack length range, it is better to carry out FEM analysis for a good precision in the electric resistance calculation if a FEM software program is available; the necessary physical and electrical properties for FEM analysis can be obtained by using the initial electric resistance and dimensions of the film.

### 3.2 Crack length measurement using rectangular ion-sputtered film

Three-point bending tests were performed for acrylic test pieces, whose crack lengths were measured using a microscope and ion-sputtered films. The test piece were 100mm in length, 10mm in depth, and 20mm in height, and the supporting span in the tests was 80mm. A V-notch was introduced into the middle of the supporting span. The load ratio $P_{min}/P_{max}$ was 0.02 and the load frequency was 10Hz. The experimental method and an ion-sputtered film on a test piece are shown in Figure 12. All tests were stopped when the crack grew to about $0.6w$ ($w$: film width) for the determination of the constant $c$ in expression (4).
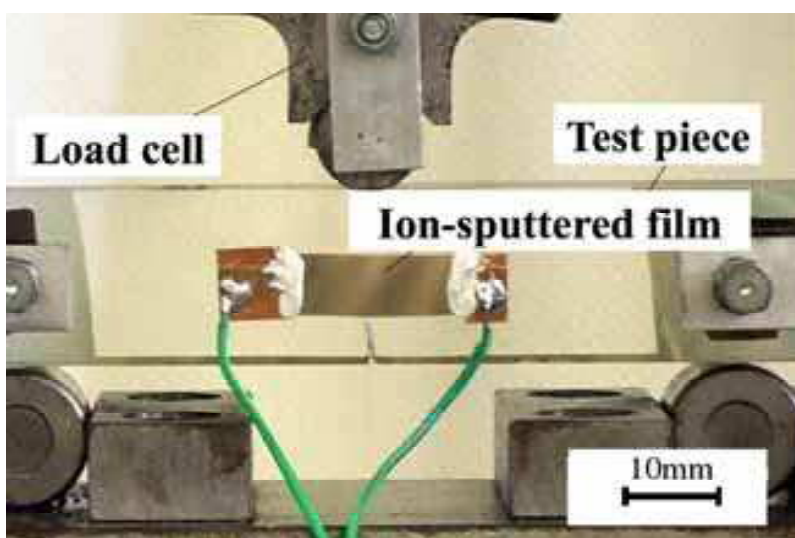


Fig. 12. Rectangular ion-sputtered film on acrylic test piece

The comparison of the crack lengths measured using an optical microscope and an ion-sputtered film is shown in Figure 13. The crack lengths are in very good agreement. Their maximum difference is 0.113mm and their average is only 0.051mm. A relatively large crack length difference occurs when the cracks are very short. This difference is considered to be due to the interruption of the experiment and taking off the test pieces form test rig for crack length measurement using an optical microscope that leads to the changes in the electrical environmental conditions around the test pieces. Although the precision of this rectangle is not as high as that of a grid pattern film, it is greatly higher than that of a commercial crack gauge (Deng et al., 1991). Therefore, a rectangular ion-sputtered film can be used to measure crack length continuously; short cracks or cracks with high growth rate, such as those in glass and ceramics, might be measurable by using a high-frequency sampling system.

## 4. Evaluation of crack growth characteristics of glass and ceramics based on crack length measurement using ion-sputtered film

It is known that fatigue failures also occur in structure components made of glass and ceramics under a constant load or a dynamic load (Hoshide, 1994). Since a small crack will

grow more unstably and crack growth rate may increases more markedly within a small stress intensity factor range in brittle materials than in ductile metals, the understanding of the small crack growth characteristics in brittle materials, such as glass and ceramics, is very important for the prediction of the residual life. Many researches have been performed to clarify the relationship between the crack growth rate and the stress intensity factor for glass and ceramics using fatigue tests (Wakai et al., 1986, Takahashi et al., 1991, Sawaki et al., 1992, Aze et al., 2002, Yoda, 1989, Kimura et al., 1987). However, most of these researches used standard test pieces, such as compact test pieces or double-torsion test pieces, where the crack length is usually over several millimeters; thus, the crack growth characteristics known up to now are considered appropriately restricted to the large cracks that are impractical in the structure components made of glass and ceramics. For investigating the growth characteristics of a small crack with a length shorter than 1mm in glass and ceramics, a high-precision and high-speed crack length measurement method is necessary. Other methods, such as microscopy observation, the compliance method, the opening displacement method and the estimation methods based on the changes in electric properties around the crack are not applicable. However, the presented crack length measurement method using an ion-sputtered film makes it possible to measure the crack growing in glass and ceramics, since the ion-sputtered film is extremely thin that its electric resistance may change owing to a small increase in crack length, and a high-speed sample system is used for recording the electric resistance of the film.
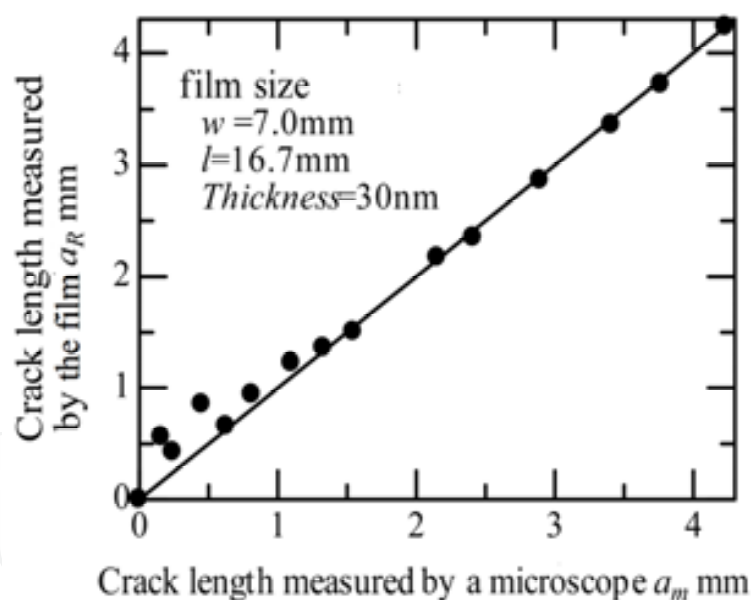


Fig. 13. Comparison of crack length obtained by microscope and ion-sputtered film

In this section, a concrete example of the application of a rectangular ion-sputtered film to clarifying small crack growth characteristics, namely, the relationship between the crack growth rate and the stress intensity factor, in soda-lime glass and alumina ceramics is discussed in detail.

### 4.1 Four-point bending test piece and fatigue test method
Four-point bending fatigue tests were performed under a constant load. The test pieces were made of soda-lime glass and alumina ceramics. The main chemical components and typical

properties of the materials are shown in Table 1. The dimensions of the test pieces are shown in Figure 14. The test piece of soda-lime glass is 100mm long, 12mm wide ($B$) and 9.6mm thick ($W$), and the test piece of alumina ceramics is 100mm long, 12mm wide and 10mm thick. A precrack was introduced at the center of the lower surface of the test piece using a diamond indenter, and the ion-sputtered film was prepared traversing the crack growth directions. The film $w$ and $l$, precrack length $c_0$, and distance $s$ were measured using an optical microscope before the fatigue tests. The measurement error in the electric resistance of the cracked film was about 2-3% for the film of $l/w$=2.0 based on the results mentioned in section 3.1.

| Material | | Soda-lime glass | | Alumina ceramics | |
|---|---|---|---|---|---|
| Main components   wt% | SiO$_2$ | 72.0 | Al$_2$O$_3$ | | 99.5 |
| | CaO | 10.0 | | | |
| | Na$_2$O | 14.0 | | | |
| Grain size          μm | | Amorphia | | 10 | |
| Young's modulus   GPa | | 71.6 | | 363 | |
| Bending strength   MPa | | 49.0 | | 441 | |

Table 1. Main chemical components and properties of the test materials
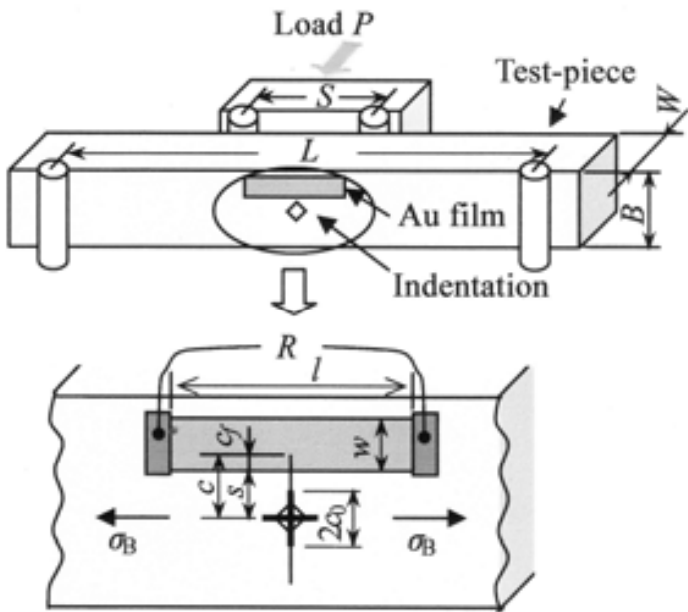


Fig. 14. Dimensions of four-point bending test piece

Static fatigue crack growth can be observed in glass and ceramic materials owing to stress corrosion. A constant load was applied to the test piece in this experiment. The loading and supporting methods are shown in Figure 14. The upper loading span ($S$) and lower supporting span ($L$) are 30mm and 90mm for the soda-lime glass, and 10mm and 25mm for

the alumina ceramics, respectively. The simple system shown in Figure 3 was used to record the voltage on the ion-sputtered film, and the electric resistance of the film was calculated with the voltage and the set values of the other components in the measurement system. Since the crack grew at a high speed in glass and ceramics under a constant load, the recording frequency was 125kHz; thus, the crack length could be measured nearly continuously.

### 4.2 Calculation of stress intensity factor for surface crack and crack growth rate

A surface crack from a diamond indenter pit takes the shape of a semi-ellipse as shown in Figure 15. The stress intensity factor varies with the position at the edge of a crack. The maximum stress intensity factor at point $A$, which is used in the following discussion, is expressed as below (Kunio et al., 1984),

$$K_I = \frac{3.3P(L-S)\sqrt{\pi c(a_0/c_0)}}{2BW^2\sqrt{1+1.46(a_0/c_0)^{1.65}}} \qquad (5)$$

here, $P$, $S$, $L$, $W$, $B$, $a_0$, and $c_0$ are the load, upper loading span, lower supporting span, test piece thickness, test piece width, initial crack length in the depth direction, and initial surface crack length, respectively. In expression (5), the crack length $a$, as shown in Figure 15, is substituted by $c(a_0/c_0)$ on the basis of the assumption that the aspect ratio $\lambda$, defined as the ratio of the crack length (depth) $a$ to the surface crack length $c$ namely, $\lambda=a/c$, is a constant during crack propagation. The aspect ratio $\lambda$ can be obtained using the initial crack length $a_0$ and $c_0$ measured in the break section after the fatigue test using an optical microscope, and $c$ is the surface crack length measured using the ion-sputtered film.
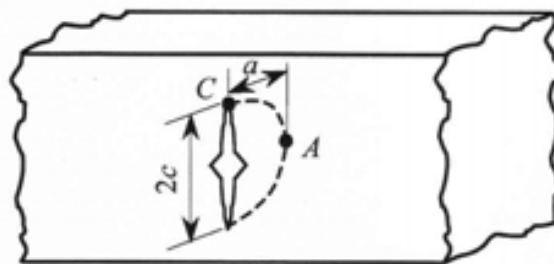


Fig. 15. Semi-ellipse surface crack

The surface crack length was derived from the electric resistance of the film based on the relationship between the crack length and the electric resistance of the ion-sputtered film obtained through the above-mentioned FEM analysis. To remove the effects of the sampling errors included in the electric resistance of the ion-sputtered film, as shown in Figure 16, on the surface crack length, the simple moving average method was used to obtain a smooth relationship between the surface crack length and the loading time, as shown in Figure 17. On the basis of the assumption that the aspect ratio $\lambda$ is constant during crack propagation, the crack length $a$ in the depth direction of the test piece was measured as the product of the surface crack length $c$ multiplied by the aspect ratio $\lambda$, namely $a=c\cdot\lambda$, and then, the crack growth rate $da/dt$ was determined by differentiating the relationship between the crack length $a$ and the loading time $t$.
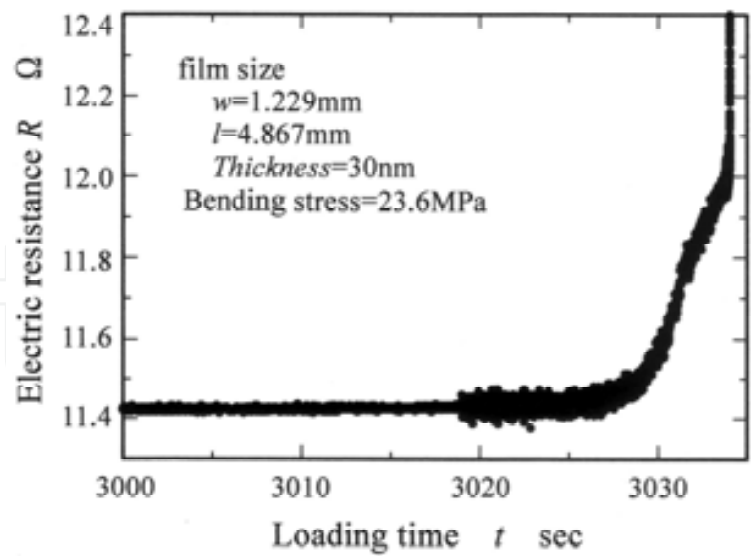
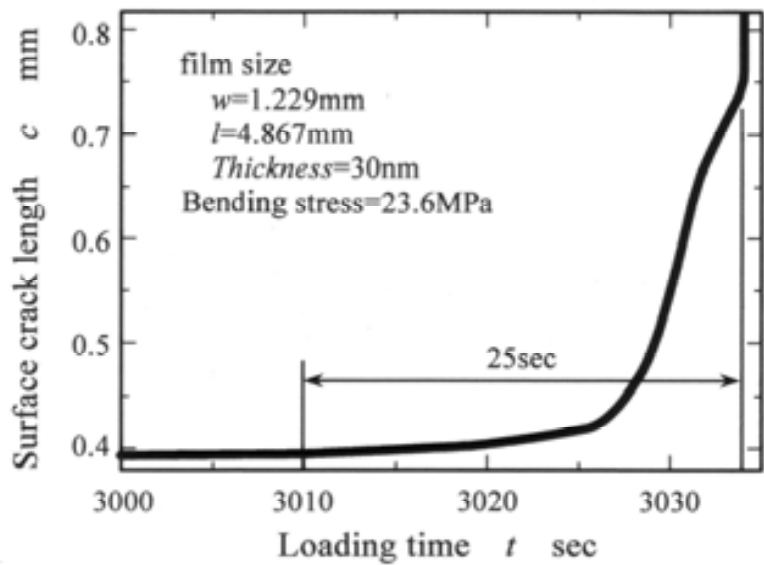Fig. 16. Electric resistance of the ion-sputtered film during fatigue test for soda-lime Glass



Fig. 17. Crack growth during fatigue test for soda-lime glass

## 4.3 Crack growth characteristics of soda-lime glass

The growth of a surface crack in the soda-lime glass test piece is shown in Figure 17. Fracture occurred when the crack length reached about 0.8mm; thus, the critical or unstable crack growth is expected to start from a small crack under a constant load. Moreover, crack growth time was about 25sec from the total fatigue time of about 3,040sec; the crack growth stage occupied less than 1% of the entire fatigue process.

Figure 18 shows the relationship between the crack growth rate and the stress intensity factor for the soda-lime glass under the bending stress of 22.8 and 23.6MPa. It has been very difficult up to now to measure the growth rate of a small crack, particularly the low and high (unstable) growth rates in brittle materials. In this experiment, since the ion-sputtered film can measure a small crack with high precision, and the sampling frequency of the

measurement systems is so high that the surface crack can be measured almost continuously, a complete relationship including the three regions of crack growth was obtained successfully. In the stress intensity range from 0.45 to 0.85MPa·m$^{1/2}$, the crack growth rate changed from very low to very high in the soda-lime glass; thus, the unstable crack growth occurs easily in the soda-lime glass under a constant load.
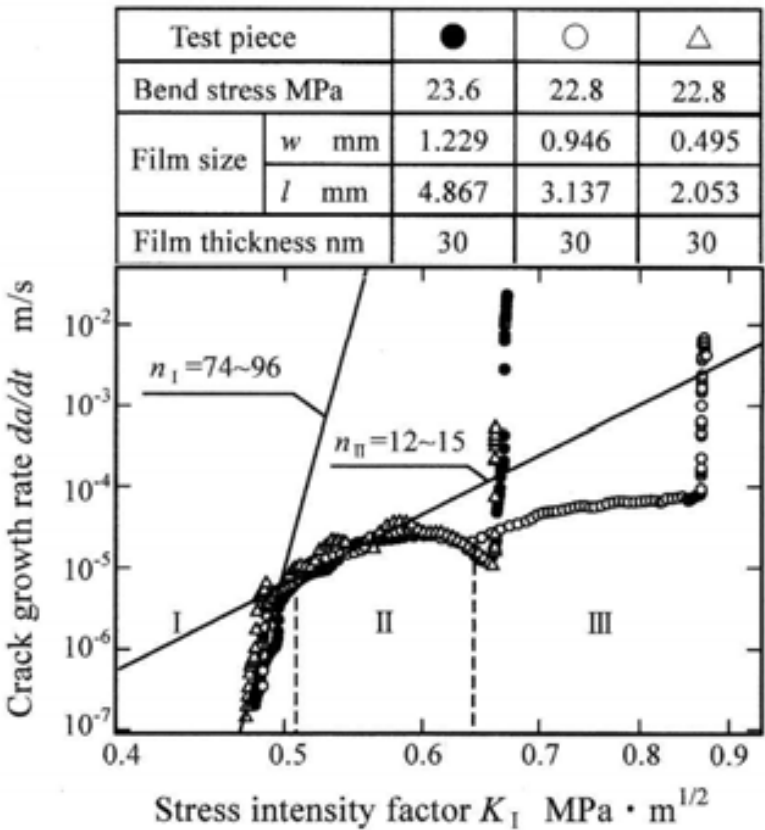
| Test piece | | ● | ○ | △ |
|---|---|---|---|---|
| Bend stress MPa | | 23.6 | 22.8 | 22.8 |
| Film size | w mm | 1.229 | 0.946 | 0.495 |
| | l mm | 4.867 | 3.137 | 2.053 |
| Film thickness nm | | 30 | 30 | 30 |



Fig. 18. Crack growth characteristics in soda-lime glass

On the basis of the Paris law indicating that the crack growth rate is proportional to the $n$th power of the stress intensity factor, that is $\frac{da}{dt} = cK_I^n$, the constant $n$ was determined to range from 74 to 96 in region I, and from 12 to 15 in region II for the soda-lime glass. Yoda (1989) and Wiederhorn (1967) obtained $n$ values ranging from 10 to 16 in the region of the crack growth rate from 1x10$^{-6}$ to 1x10$^{-4}$, which agree with those obtained in region II of this experiment. The results of this experiment consequently clarify the crack growth characteristics of the soda-lime glass not only in region II but also in regions I and III; the crack length measurement method using a rectangular ion-sputtered film might be practical for investigating the crack growth characteristics of brittle materials, such as soda-lime glass.

## 4.4 Crack growth characteristics of alumina ceramics

The surface crack lengths measured during the test for alumina ceramics are shown in Figure 19. Brittle fracture occurred when the crack length reached about 0.55mm; thus, the critical or unstable crack growth is expected to start from a small crack under a constant

load. Moreover, crack growth time was about 130sec from the total fatigue time of about 15,760sec; the crack growth stage occupied less than 1% of the entire fatigue process.
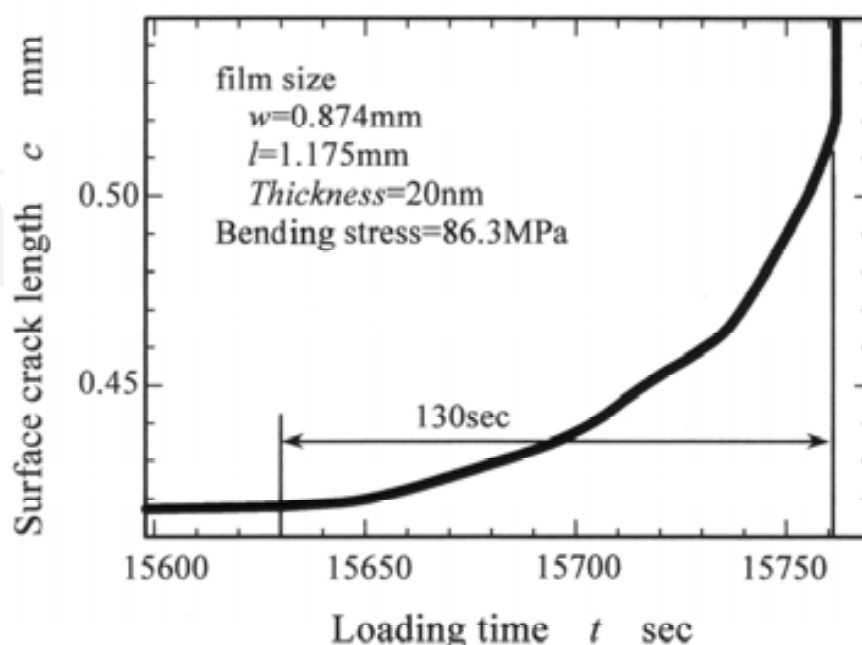


Fig. 19. Crack growth during fatigue test for alumina ceramics

Figure 20 shows the relationship between the crack growth rate and the stress intensity factor for the alumina ceramics under the bending stress of 86.3MPa. The surface crack length was also measured almost continuously, resulting in the successful determination of a complete relationship in the three regions of crack growth. The stress intensity factors range where the crack growth rate changes from low to high (unstable) in the alumina ceramics is very small (about 0.2 to 0.4 MPa·m$^{1/2}$), which is similar to that of soda-lime glass; thus, the unstable crack growth occurs easily under a constant load. On the basis of the fact that the stress intensity factor for the crack growth in alumina ceramics is much higher than that in the soda-lime glass, alumina ceramics are considered to have a much higher fatigue strength than soda-lime glass.

Considering that the $n$ values range from 530 to 580 in region I, and from 17 to 25 in region II for the alumina ceramics, the crack growth rate increases markedly owing to the small increase in stress intensity factor, particularly in region I. The $n$ values obtained by Wakai et al. (1986) using double-torsion test pieces range from 84 to 130 in the crack growth rate range of $2 \times 10^{-7}$ to $1 \times 10^{-3}$, which is different from those obtained in this experiment. Considering that the crack lengths in this experiment are below 1mm, much shorter than those in the experiments of Wakai et al., the difference in $n$ might be due to the fact that the crack growth characteristics depend on crack length.

The circle in region II in Figure 20 also indicates a decrease in crack growth rate. The shapes of the surface cracks in the soda-lime glass and alumina ceramics are observed using a microscope and shown in Figure 21. The crack grew linearly in the soda-lime glass but meandered in the alumina ceramics. Since the ion-sputtered film can only measure the crack length in the traversing direction of the film, the meandering of the crack would be seen as a decrease in crack growth rate.
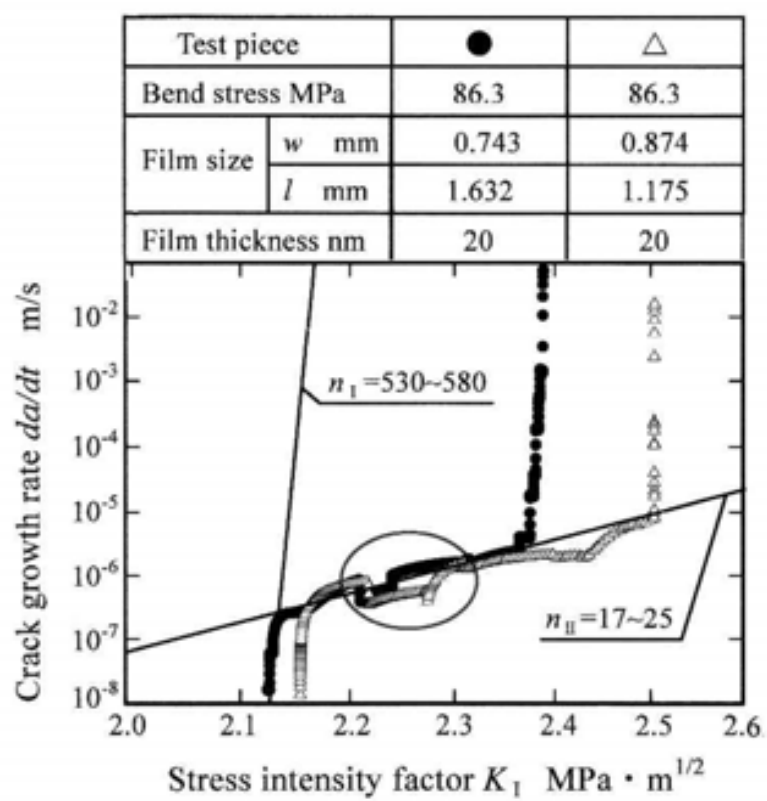
| Test piece | | ● | △ |
|---|---|---|---|
| Bend stress MPa | | 86.3 | 86.3 |
| Film size | $w$ mm | 0.743 | 0.874 |
| | $l$ mm | 1.632 | 1.175 |
| Film thickness nm | | 20 | 20 |

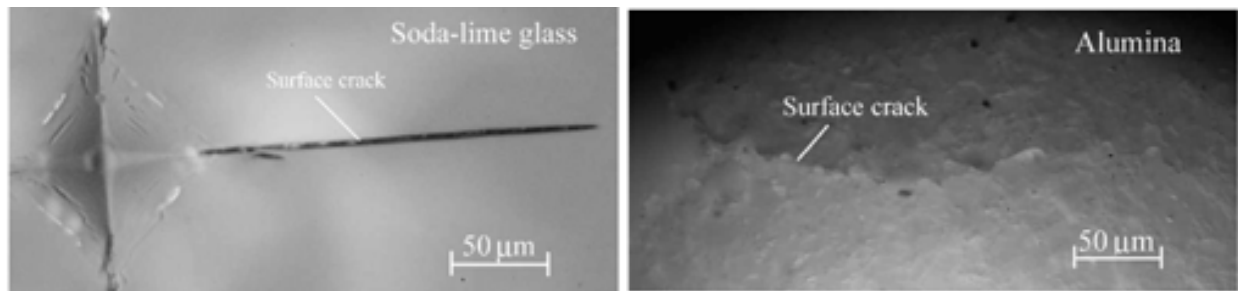Fig. 20. Crack growth characteristics in alumina ceramics

Fig. 21. Appearances of surface cracks in soda-lime glass and alumina ceramics

## 5. Application of crack length measurement using ion-sputtered film to metal surface

Ion-sputtered films can also be applied to crack length measurement for a metal surface if an insulating film could be fabricated between an ion-sputtered film and a metal surface. The insulating film should be as thin as possible for a high measurement precision. Many methods, such as the vacuum evaporation of silicon and glass, spray pyrolysis using ZnO, painting with quick-drying glue (Krazy Glue) and varnishing using an insulating spray paint, have been used to fabricate a thin insulating film on a steel surface. The method of varnishing using an insulating spray paint was selected finally for the high insulating resistance, thinness and fabrication convenience. The spray paint used in this experiment is the coating agent AY-302 (Sunhayato Co., Tokyo, Japan), which is commonly used in the insulation of printed circuit boards. The main component of the coating agent is polyvinyl

resin. Wiping the steel surface with absorbent cotton wetted with the coating agent produces a good-quality and thin isolating film of about 1-2μm thickness. The insulating electric resistance between the ion-sputtered film and the steel surface was measured; its value was as high as several hundreds of ohm for an ion-sputtered film of about 5mm×10mm.

A sectional view of the insulating film, the ion-sputtered film and the wring method used for the crack length measurement on a steel test piece are shown in Figure 22. The insulating film should be fabricated after the setting of the terminal and wiring, and the ion-sputtered film should be fabricated immediately before the experiment.
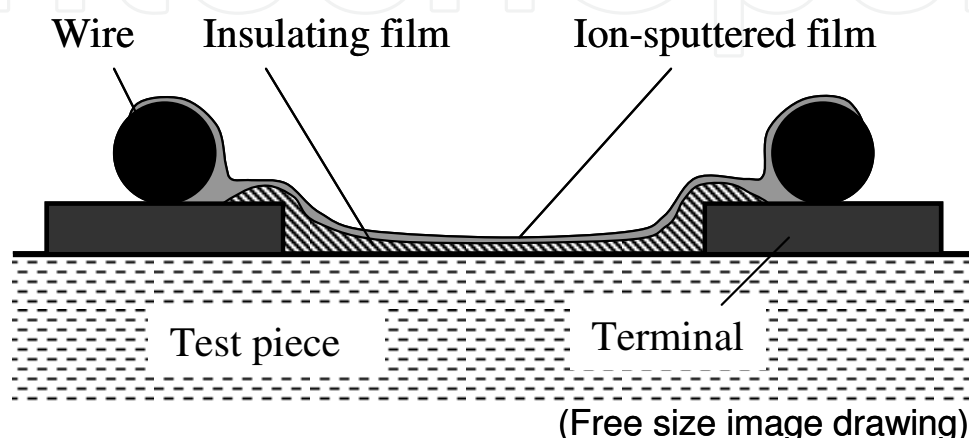


Fig. 22. Method applying ion-sputtered film to metal surface

## 6. Fatigue crack initiation detection method using ion-sputtered film

Many studies have been performed on the detection method for fatigue crack initiation that is very important in the evaluation of fatigue strength. Makabe et al. (1992, 1994a, 1994b) used a strain waveform for the detection of a fatigue crack with a length of 0.5 to 1mm on a round test piece with a small hemispherical pit. Katayama et al. (1996) and Lee et al. (2002) detected crack initiation using an AC potential method on a sharply notched test piece. Tohmyoh et al. (2001) detected the fatigue crack initiation of a test piece with a surface slit during rotating bending tests using surface SH (shear-horizontal) waves. Papazian et al. (2007) and Zilberstein et al. (2001, 2003, 2005) performed many studies on the application of a meandering winding magnetometer array sensor, ultrasonic techniques and an electrochemical fatigue sensor for the detection of crack initiation for many different types of fatigue test pieces. In addition to the above-mentioned methods, since the ion-sputtered film is very thin, a very short crack can change the electric resistance of the ion-sputtered film; thus, the ion-sputtered film would be practical for detecting the instant of fatigue crack initiation during a fatigue test.

### 6.1 Principle of fatigue crack initiation detection method

The ion-sputtered film is as thin as several tens of nanometers; thus, a small surface crack is expected to crack the film and change the electric resistance of the film, as shown in Figure 23. The starting point of the increase in electric resistance corresponds to the instant of crack initiation.
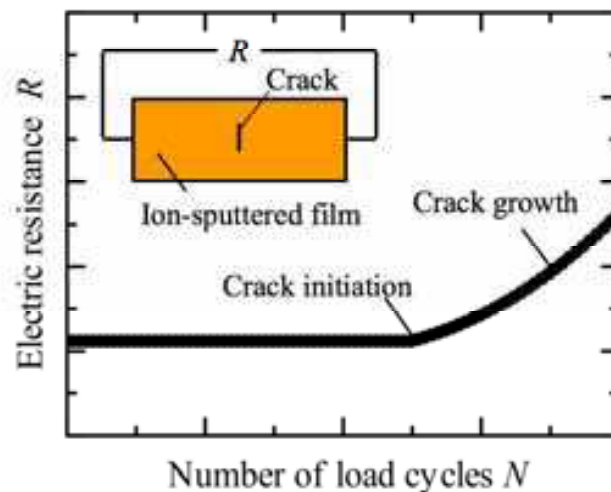
Fig. 23. Change in electric resistance of ion-sputtered film due to crack initiation and crack growth

### 6.2 Test piece for fatigue crack initiation detection

Three-point bending fatigue tests were performed to investigate the effectiveness of the ion-sputtered film in crack initiation detection. Considering that the crack initiates from stress concentration regions in machine elements, such as shafts and gears, and the convenience of fabricating an ion-sputtered film, the notch in the test piece should be round instead of being V- or U-shaped. The notches of the test pieces were in the shape shown in Figure 24, and crowned so that the crack could initiate at their centers. The test pieces were 100mm long, 10mm thick and 20mm high, and the supporting span in the tests was 80mm. The radius of the round notch was 4mm, the depth of the notch top $T$ was about 5mm and the crowning radius $R$ was about 5mm.

The test pieces were made of acrylic. The ion-sputtered film was formed on the notch surface. The length of the film in the direction of the test piece length was about 10mm, and the width and the thickness of the film were about 5mm and 10-50nm, respectively. The initial electric resistance of the film was lower than 20ohm. As shown in Figure 3, the system was used to record the voltage on the ion-sputtered film.
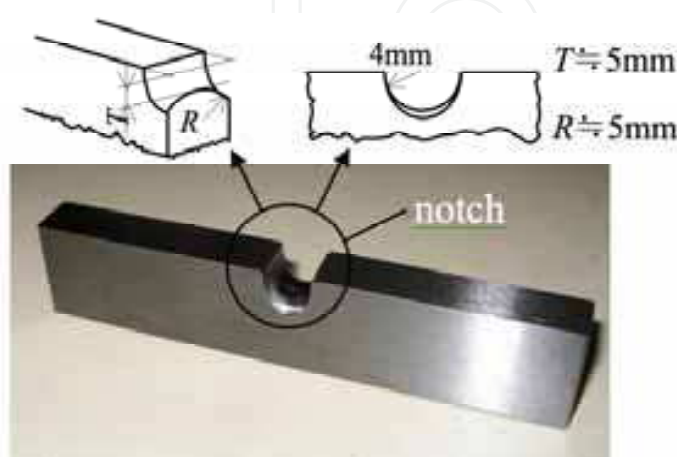


Fig. 24. Test piece for crack initiation detection test

## 6.3 Durability of ion-sputtered film

Whether the change in electric resistance or physical damage to the film occurs during the fatigue test before crack initiation was investigated to confirm the suitability of the film. The film was subjected to an endurance test under a light load without fatigue breaks. Figure 25 shows the electric resistance of the film during the test. It is obvious that no physical damage occurred in the film during the test, although a slow decrease in the electric resistance of about 0.5ohm was observed under load cycles of $1 \times 10^7$ (about 90hr). Gradual changes in electric resistance also occurred during some of the subsequent experiments; the reasons for these changes have not yet been clarified. However, considering that the film was made of pure gold (Au) without deteriorations of material properties due to chemical reactions under these test conditions, and that the changes were much slower than that due to crack initiation, the gradual changes might be caused by some unknown environmental factors or the electric shifts of the apparatuses in the measurement system. On the basis of the above-mentioned results, the gradual changes are considered not so severe that the judgment of crack initiation is prevented.

## 6.4 Change in electric resistance due to crack initiation

The electric resistance of the ion-sputtered film on an acrylic test piece during the fatigue test is shown in Figure 26. The maximum load was 400N, the loading frequency was 10Hz and the film thickness was about 30nm. The experiment was stopped manually after recognizing a rapid increase in voltage signal on the monitor of the data recorder. Figure 26 clearly shows an increase in the electric resistance of the film, indicating crack initiation. Despite the fact that gradual changes in the electric resistance of the film sometimes occur, as shown in Figure 25, the increase in electric resistance due to crack initiation is clear compared with the gradual changes shown in Figure 25, and the crack initiation point can be confirmed from Figure 26 by observing the upward tendency of the electric resistance. The point where the electric resistance leaves the extension line of the mean electric resistance is considered to be the start point of crack initiation. The notch after the experiment is shown in Figure 27, and a very small round crack, the crack in the primary stage of fatigue, can be observed clearly.
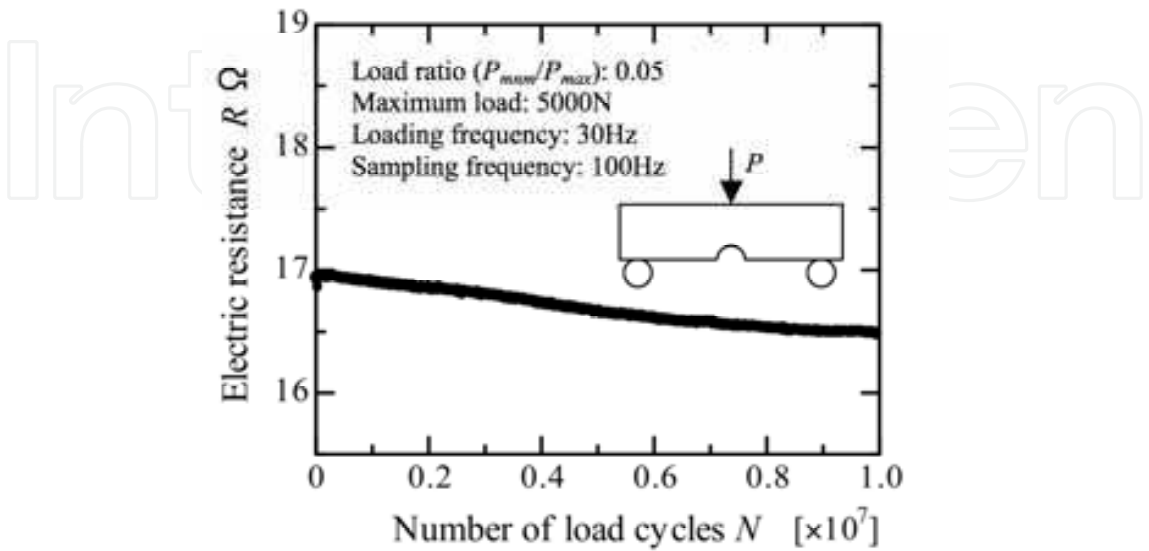


Fig. 25. Electric resistance of ion-sputtered film during the test without crack initiation
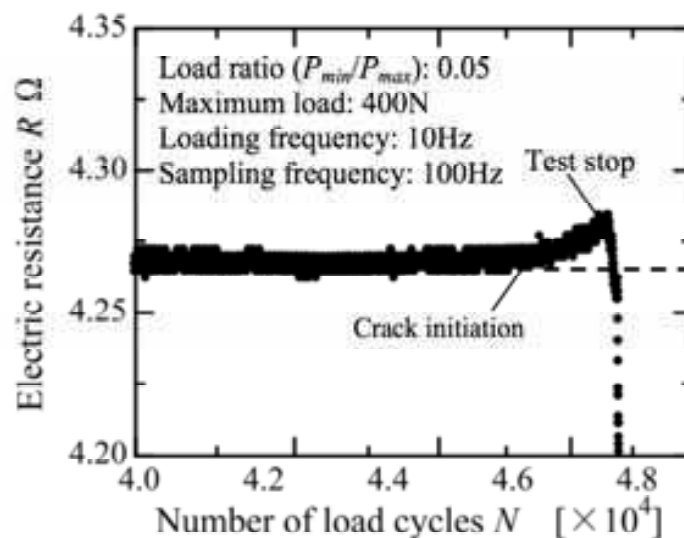
Fig. 26. Change in electric resistance of ion-sputtered film when fatigue crack initiation
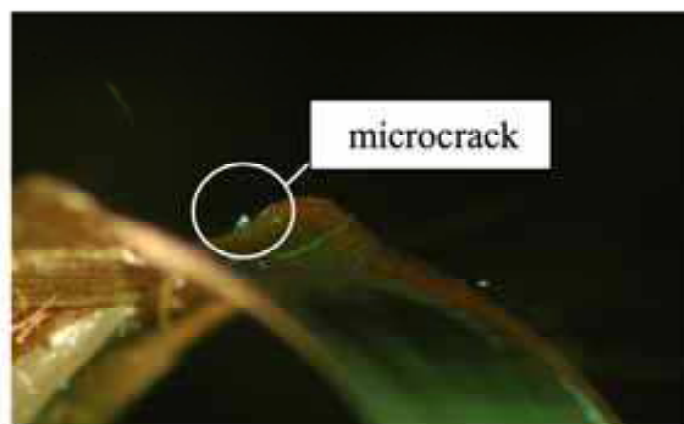


Fig. 27. View of micro-crack initiated on notch surface

## 6.5 Shape of detected crack in primary stage of fatigue

A small sample around the notch was quarried out from the test piece to determine the crack front shape. The sample was cut bit by bit from the side using a milling machine. The depth of the sample $d$ and the crack length $a$ on the side surface were measured using a micrometer and an optical microscope, respectively. The shape of the crack front is shown in Figure 28. It can be seen that the shape of the crack front is approximately half an ellipse, the length of the crack on the notch surface is about 0.35mm and the maximum depth is about 0.2mm. The half ellipse shape indicates that the crack is in the primary stage of fatigue. It is slightly difficult to say that the crack shown in Figure 28 is the just-initiated crack since the dimensions of the crack are rather large. The large dimensions are due to the time lag between the judgment of crack initiation from the change in electric resistance and the termination of the test, not due to the sensitivity of the ion-sputtered film because the measurement error of the film is as small as 0.068mm (Deng et al., 2007). From the change in the electric resistance of the ion-sputtered film and the shape of the detected crack shown in

Figures 26, 27 and 28, it can be concluded that the ion-sputtered film can be used to detect the initiation of a fatigue crack. Considering the convenience to prepare the detecting system, this method is simple and practical for monitoring fatigue crack initiation.
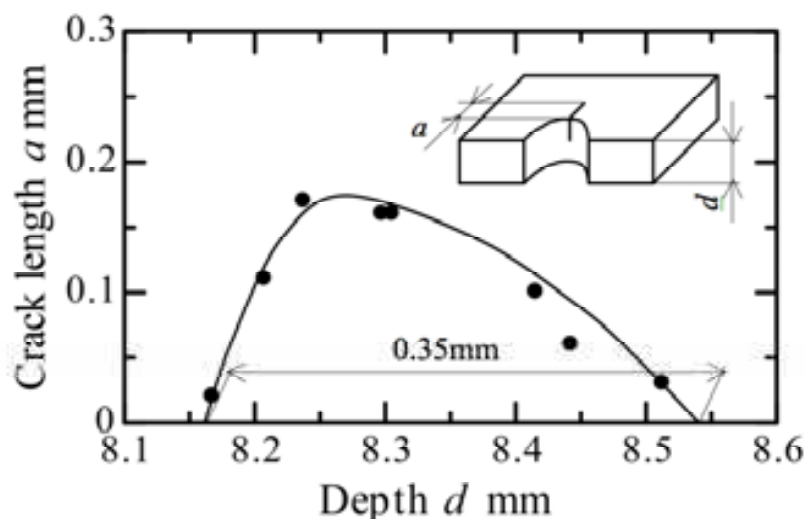


Fig. 28. Shape of crack initiated in acrylic test piece

## 7. Conclusions

The methods for crack length measurement and fatigue crack initiation detection using an ion-sputtered film based on the changes in the electric resistance of the film due to crack growth or crack initiation are presented. On the basis of that the experimental results of crack length measurement and crack initiation detection, and considering the convenience to prepare the measurement and monitoring systems, the presented methods are very practical for investigating crack growth characteristics and crack initiation life.

One of the crack length measurement methods is the use of a grid pattern ion-sputtered film, which is similar to a crack gauge. Since the electric resistance of the film changes only at the point when a grid is entirely snapped by a crack, the calculation of the electric resistance is not necessary, the crack length can be obtained by counting the number of increasing steps in the recorded electric resistance and measuring the positions of the grids. Because the thickness of the ion-sputtered film is only several tens of nanometers, the change in the electric resistance of the film due to grid snapping is more immediate than that of the commercial crack gauge. Grid pattern ion-sputtered films were applied to the crack length measurement for a three-point bending test piece. Very obvious staircase changes in the electric resistance of the film were recorded.

Another crack length measurement method is the use of a rectangular ion-sputtered film, which can measure crack length continuously. The relationship between the electric resistance of the film and crack length is obtained by electrothermal FEM analysis, and an approximate expression is proposed to calculate the electric resistance of a cracked film using the results of electrothermal FEM analysis. Since the film is extremely thin, it is very sensitive to the increase in the length of a small crack and practical for investigating a small crack with high growth rate. As the application of the crack length measurement method using a rectangular ion-sputtered film, cracks in soda-lime glass and alumina ceramics were

measured and the crack growth characteristics in these materials were clarified continuously from the crack growth region I to the crack growth region III.

In addition to crack length measurement, an ion-sputtered film can also be applied to the detection of fatigue crack initiation, which is a very important technique for evaluating the fatigue strength of a material. Since the film is extremely thin and can be fabricated directly on a surface, a very small crack can change its electric resistance. As an attempt to confirm the fatigue crack initiation life, an ion-sputtered film was formed on the round notch surface of a three-point bending acrylic test piece; a very small crack that initiated from the notch surface during the fatigue test was detected. From the change in the electric resistance of the ion-sputtered film during the test and the shape of the detected crack, it can be concluded that the ion-sputtered film can be used to detect the initiation of a fatigue crack.

## 8. References

Ashida, U., Ishihara, T., Fujihara, H. & Tobita, H. (1996). Automatic Measurement of Fatigue Crack Length by a D.C. Electrical Potential Difference Method, *Journal of The Kansai Society of Naval Architects (in Japanese)*, 225, 181-185

Aze, A.D., Chevalier, J., Fantozzi, G., Schehl, M. & Torrecillas, R. (2002). Crack Growth Resistance of Alumina, Zirconia and Zirconia Toughened Alumina Ceramics for Joint Prostheses, *Biomaterials*, Vol.23, No.3, 937-945

Brown, T.F. & Srawley, J.E. (1966). In Plane Strain Crack Toughness Testing of High Strength Metallic Materials, *ASTM STP410*

Bucci, R.J., Paris, P.C., Hertzberg, R.W., Scbmidt, R.A. & Anderson, A.F. (1972). Fatigue Threshold Crack Propagation in Air and Dry Argon for a Ti-6Al-4V Alloy, *ASTM STP513*, 125-140

Deng, G., Inoue, K., Takatsu, N. & Kato, M. (1991). Evaluation of the Strength of Carburized Spur Gear Teeth Based on Fracture Mechanics, *Trans. Jpn. Soc. Mech. Eng. (in Japanese)*, C-57-535, 909-913

Deng, D., Tokunaga, H., Daniel-Redda, T., Ikeda, K., Nakanishi, T. & Kaizu, K. (2006). Crack Length Measurement with an Ion Sputtered Film, *Trans. Jpn. Soc. Mech. Eng. (in Japanese)*, 72-715, 997-1002

Deng, D., Nasu, K., Kuroia, S. & Nakanishi, T. (2007). Crack Length Measurement with an Ion Sputtered metal Film, *Trans. Jpn. Soc. Mech. Eng. (in Japanese)*, 73-727, 849-854

Hoshide T. (1994). Fatigue in Ceramics I, *Journal of The Society of Materials Science*, Vol.43, No.490, 902-908

James, L.A. (1981). Specimen Size Considerations in Fatigue Crack Growth Rate Testing, *ASTM STP738*, 45-57

JSME (1986). JSME Standard, *Jpn. Soc. Mech. Eng.*, S-001, 8-9

Katayama, Y., Sakane, M. & Ohnami, M. (1996). Surface Crack Detection by A. C. Potential Drop Method; Experiment and FEM Considerations, *Trans. Jpn. Soc. Mech. Eng. (in Japanese)*, Vol.62-602, 2216-2223

Kimura, Y., Yamamoto, S., Sekiya, M. & Kunio, T. (1987). Crack Growth Characteristics of Vickers Indented Glass Plate Specimen in Water, *Journal of The Society of Materials Science*, Vol.36, No.401, 160-165

Kunio, T., Nakazawa, K., Hayashi, I. & Okamura, H. (1984). *(Methods for Fracture Mechanics), (in Japanese)* , 251-252

Lee, J.H. & Kobayashi, H. (1985). Detection and Closure Measurement of Short Fatigue Crack Initiated at Notch Root, *Trans. Jpn. Soc. Mech. Eng. (in Japanese)*, A-51-461, 142-147

Lee, Y. & Sakane, M. (2002). Multiple Surface Crack Detection Using A. C. Potential Drop Method, *Trans. Jpn. Soc. Mech. Eng. (in Japanese)*, Vol.68-672, 1220-1227

Makabe, C., Nishida, S., Kaneshiro, H. & Tamaki, S., (1992). Method of Detecting Fatigue Crack Initiation through Analysis of Strain Waveform, *Trans. Jpn. Soc. Mech. Eng. (in Japanese)*, Vol.58-551, 1191-1195

Makabe, C., Kaneshiro, H., Nishida, S. & Urashima, C. (1994a). Detection of 1mm Fatigue Crack Initiation Using Strain Waveform, *Journal of engineering Materials and technology, Trans. of ASME*, Vol.116, 483-487

Makabe, C., Nishida, S., Urashim, C. & Kaneshiro, H. (1994b). Detection of Fatigue Crack Initiation under a Random Load, *Trans. Jpn. Soc. Mech. Eng. (in Japanese)*, Vol.60-576, 1753-1760

Masuyama, T., Inoue, K. & Kato, M. (1994). Acoustic Emission during Fatigue Crack Growth in Carburized Gear Tooth, *Trans. Jpn. Soc. Mech. Eng. (in Japanese)*, C-60-575, 2456-2461

Mautz, J. & Weiss, V. (1976). Mean Stress and Environmental Effects on Near Threshold Fatigue Crack Growth, *ASTM STP601*, 154-168

Nakai, Y., Akagi, H., Kitamura, Y. & Ohji, K. (1989). Measurement of Short Surface Crack Length by an AC Potential Method, *Trans. Jpn. Soc. Mech. Eng. (in Japanese)*, A-55-511, 543-548

Nakamura, M., Saitoh, K., Ikeyama, M., Kozuka, T. & Shigematsu, I. (1993). A Study on the Utilization of an Electro-Conductive Surface Layer on a $Si_3N_4$ Ceramic Formed by Ion Implantation as a Crack Gage and a Strain Gage, *Journal of the Ceramic Society of Japan (in Japanese)*, 101-1, 139-142

Nishitani, H. & Chen, D. (1985). A Consideration on the Unloading Elastic Compliance Method, *Trans. Jpn. Soc. Mech. Eng. (in Japanese)*, A-51-465, 1436-1441

Ogawa, T. & Suresh, S. (1991a). Surface Film Technique for Crack Length Measurement in Nonconductive Brittle Materials: Calibration and Evaluation, *Engineering Fracture Mechanics*, Vol.39-4, 629-640

Ogawa, T. (1991b) Fracture Resistance Curve and Fatigue Crack Growth in Polycrystalline Magnesia, *Trans. Jpn. Soc. Mech. Eng. (in Japanese)*, A-57-535, 492-499

Papazian, J. M., Nardiello, J., Silberstein, R., Welsh, G., Grundy, D., Craven, C., Evans, L., Goldfine, N., Michaels, J.E., Michaels, T.E., Li, Y. & Laird, C. (2007). Sensors for Monitoring Early Stage Fatigue Cracking, *International Journal of Fatigue*, Vol.29, 1668-1680

Sawaki, Y., Nagase, Y., Yoshida, H., Inoue, A. & Fujiwara, T. (1992). Crack Propagation Behaviour in Alumina Ceramics under Static and Cyclic Loading, *Trans. Jpn. Soc. Mech. Eng., Series A*, Vol.58, No.552, 1333-1338

Shimada, H. & Date, K. (1983). Crack Depth Measurement with High Accuracy by Ultrasonics, *The Iron and Steel Institute of Japan (in Japanese)*, 69-2, 196-202

Takahashi, M. & Mutoh, Y. (1991). Static and Cyclic Fatigue Crack Growth in Several Ceramic Materials, *Trans. Jpn. Soc. Mech. Eng., Series A*, Vol.57, No.543, 2615-2621

Tohmyoh, H., Ochi, Y. & Matsumura, T. (2001). Study on Detection and Quantitative Evaluation of Fatigue Cracks Using Surface SH Waves, T*rans. Jpn. Soc. Mech. Eng. (in Japanese)*, Vol.67-661, 1508-1513

Tokunaga H., Ikeda K., Kaizu K. & Kinishita H. (2007). Micro-Crack Length Measurement Method in Ceramics by Using Grid Pattern Metal Film, *CD Proceedings of International Conference an Advanced Experimental Mechanics 2007*, 1-5

Wakai, F., Sakuramoto, H., Sakaguchi, S. & Matsuno, Y. (1986). Evaluation of Crack Propagation in Ceramics by Double-Torsion, *Journal of The Society of Materials Science*, Vol.35, No.395, 898-903

Wiederhorn, S. M. (1967). Influences of Water Vapor on Crack Propagation in Soda-lime Glass, *Journal of American Ceramics Society*, 50(8), 407-414

Yoda, M. (1989). Subcritical Crack Growth Characteristics of Soda-Lime Glass Evaluated from CT Specimen and Bend Specimen with Small Indented Crack, *Journal of the Ceramic Society of Japan*, Vol.97, No.9, 960-964

Zilberstein, V., Schlicker, D., Walrath, K., Weiss, V. & Goldfine N. (2001). MWM Eddy Current Sensors for Monitoring of Crack Initiation and Growth During Fatigue Tests and In Service, *International Journal of Fatigue*, Vol.23, S477-S485

Zilberstein, V., Walrath, K., Grundy, D., Schlicker, D., Goldfine, N., Abramovici, E. & Yentzer, T. (2003). MWM Eddy-current Arrays for Crack Initiation and Growth Monitoring, *International Journal of Fatigue*, Vol.25, 1147-1155

Zilberstein, V., Grundy, D., Weiss, V., Goldfine N., Abramovici, E., Newman, J. & Yentzer, T. (2005). Early Detection and Monitoring of Fatigue in High Strength Steels With MWM-Arrays, *International Journal of Fatigue*, Vol.27, 1644-1652
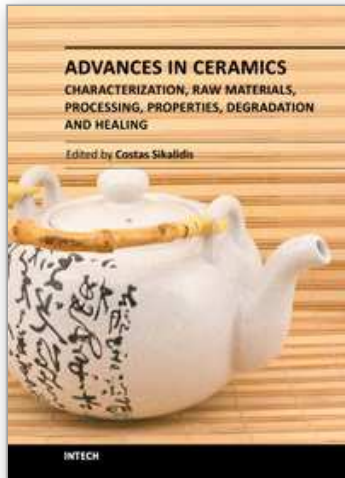
**Advances in Ceramics - Characterization, Raw Materials,**
**Processing, Properties, Degradation and Healing**
Edited by Prof. Costas Sikalidis

The current book consists of eighteen chapters divided into three sections. Section I includes nine topics in characterization techniques and evaluation of advanced ceramics dealing with newly developed photothermal, ultrasonic and ion spattering techniques, the neutron irradiation and the properties of ceramics, the existence of a polytypic multi-structured boron carbide, the oxygen isotope exchange between gases and nanoscale oxides and the evaluation of perovskite structures ceramics for sensors and ultrasonic applications. Section II includes six topics in raw materials, processes and mechanical and other properties of conventional and advanced ceramic materials, dealing with the evaluation of local raw materials and various types and forms of wastes for ceramics production, the effect of production parameters on ceramic properties, the evaluation of dental ceramics through application parameters and the reinforcement of ceramics by fibers. Section III, includes three topics in degradation, aging and healing of ceramic materials, dealing with the effect of granite waste addition on artificial and natural degradation bricks, the effect of aging, micro-voids, and self-healing on mechanical properties of glass ceramics and the crack-healing ability of structural ceramics.

**How to reference**

In order to correctly reference this scholarly work, feel free to copy and paste the following:

Gang Deng and Tsutomu Nakanishi (2011). Practical Methods for Crack Length Measurement and Fatigue Crack Initiation Detection Using Ion-Sputtered Film and Crack Growth Characteristics in Glass and Ceramics, Advances in Ceramics - Characterization, Raw Materials, Processing, Properties, Degradation and Healing, Prof. Costas Sikalidis (Ed.), ISBN: 978-953-307-504-4, InTech, Available from:

http://www.intechopen.com/books/advances-in-ceramics-characterization-raw-materials-processing-properties-degradation-and-healing/practical-methods-for-crack-length-measurement-and-fatigue-crack-initiation-detection-using-ion-sput

INTECH
open science | open minds

www.intechopen.com

www.intechopen.com